

# Validating Mixed-Phase Cloud Optical Depth Retrieved From Infrared Observations With High Spectral Resolution Lidar

David D. Turner and Edwin W. Eloranta

**Abstract**—Single-layer mixed-phase clouds are prevalent in the Arctic atmosphere. The properties of mixed-phase clouds, including the optical depth of both the liquid and ice components, can be retrieved from spectrally resolved infrared radiance observations that are made in both the 8–13- $\mu\text{m}$  and 17–24- $\mu\text{m}$  windows. The accuracy of the retrieved properties from this algorithm has been established in single-phase clouds (i.e., clouds that contain only liquid or only ice) but not in mixed-phase clouds. A polarization-sensitive high spectral resolution lidar (HSRL) was deployed to the Atmospheric Radiation Measurement Program's Barrow, Alaska site during the fall of 2004. The HSRL measures optical depth directly, and the phase can be discriminated using the depolarization ratio measured by the lidar. Comparisons of the infrared retrieved optical depths with the optical depths directly observed by the lidar in clouds that consist of supercooled liquid layers precipitating ice are in good agreement, with the slope and correlation being 1.055 and 0.65 for the ice portion of the mixed-phase cloud and 0.954 and 0.82 for the liquid portion.

**Index Terms**—Atmospheric measurements, clouds, infrared measurements.

## I. INTRODUCTION

CLOUDS are an important modulator of the energy budget of the planet. The impact of clouds on the radiative fluxes, both at the surface and top of the atmosphere as well as the redistribution of the radiant energy in the atmosphere, depends first on whether a cloud is present, second on the fraction of the sky that is covered by clouds, and third by the phase and optical depth of the clouds. While there are numerous approaches to characterizing the optical depth of ice- or liquid-only clouds from ground-based remote sensors ([1] and [2], respectively), there are relatively few ground-based techniques for mixed-phase clouds [3]. Furthermore, these mixed-phase techniques are considerably younger than the single-phase techniques, and detailed evaluations of them are required.

Here, we investigate the accuracy of the mixed-phase cloud retrieval algorithm (MIXCRA [4]), which retrieves the op-

tical depth of both ice and liquid portions of single-layer mixed-phase clouds from spectrally resolved infrared radiance observations from the Atmospheric Emitted Radiance Interferometer (AERI) using observations from a state-of-the-art high spectral resolution lidar (HSRL). This comparison was performed using the data collected during the Mixed-Phase Arctic Cloud Experiment (M-PACE [5]) at the Atmospheric Radiation Measurement (ARM) North Slope of Alaska (NSA) climate research facility in Barrow, AK [6], in the fall of 2004.

The AERI is a facility instrument at the NSA site, and thus, the MIXCRA retrievals are available for multiple years from this site. The HSRL was only at the NSA site during the M-PACE. Thus, this validation effort will characterize the accuracy of the MIXCRA ice and liquid optical depths in mixed-phase clouds and, thus, provides confidence in the long record of MIXCRA values. Accurate long time series of cloud properties are critical in order to understand cloud-radiation feedback mechanisms, the impact of changing atmospheric and cloud properties on surface properties, and how the clouds in the Arctic are changing with time.

## II. METHODS

### A. MIXCRA

The MIXCRA algorithm uses an optimal estimation-based approach to retrieve the optical depth of the liquid and ice components, along with the effective radius of the liquid and ice particles, from infrared radiance observations in single-layer mixed-phase clouds [4]. The differences in the absorption coefficients of ice and liquid water across the infrared spectrum, where ice is more absorbing than liquid at 12  $\mu\text{m}$  and the opposite is true at 18  $\mu\text{m}$ , allow the algorithm to discriminate between the two phases of the cloud [4], [7].

The primary input to the MIXCRA retrieval algorithm is the infrared radiance observations from the AERI. The AERI at the NSA site is a passive hardened interferometer that measures downwelling infrared radiance at 1-cm<sup>-1</sup> resolution from 400 to 3000 cm<sup>-1</sup> (25–3.3  $\mu\text{m}$ ). Two well-characterized blackbodies, as well as corrections for nonlinearity of the detector and instrument self-apodization, yield radiance observations that are accurate to better than 1% of the ambient radiance [8], [9]. During the M-PACE, the AERI provided a 12-s averaged sky radiance spectrum every 25 s, with periodic gaps of less than 1 min when the instrument was viewing the calibration

Manuscript received October 1, 2007; revised November 19, 2007. This work was supported by the U.S. Department of Energy, Office of Science, Office of Biological and Environmental Research, Environmental Sciences Division as part of the ARM program under Grants DE-FG02-06ER64167 and DE-FG02-06ER64187. Construction of the HSRL was supported by the National Science Foundation under Grant OP-9910304.

The authors are with the Space Science and Engineering Center, University of Wisconsin—Madison, Madison, WI 53706 USA (e-mail: dturner@ssec.wisc.edu).

Digital Object Identifier 10.1109/LGRS.2008.915940

TABLE I  
SPECTRAL INTERVALS USED IN MIXCRA (IN INVERSE CENTIMETERS)

495.5 – 498.0	872.2 – 877.5
529.9 – 531.5	898.2 – 905.4
558.5 – 562.0	1092.1 – 1098.8
828.3 – 834.6	1113.3 – 1116.6
842.8 – 848.1	1142.2 – 1148.0
860.1 – 864.0	0.794 (23.8 GHz)
	1.047 (31.4 GHz)

blackbodies. The data utilized here were not processed with the recently developed principal component base noise filter [10] because MIXCRA utilizes radiance observations in “microwindows” that exist between absorption lines, and thus, the radiance observations can be averaged over small spectral intervals to increase the signal-to-noise ratio. See Table I for spectral regions used by the MIXCRA algorithm.

The MIXCRA algorithm has been incrementally improved since its original inception with the addition of observations in the 2400–2800-cm<sup>-1</sup> (3–4- $\mu$ m) band [11] and brightness temperatures at 23.8 and 31.4 GHz from a collocated microwave radiometer [12] to help constrain the retrieval. This updated algorithm was extensively validated in single-layer warm liquid water clouds over Pt. Reyes, CA [12]. However, due to the low solar elevations even near solar noon (during this intercomparison period, the maximum solar elevation was less than 4°), the 3–4- $\mu$ m observations were not used in the retrievals shown here. The brightness temperatures from the microwave radiometer that are utilized here have been bias corrected using the approach in [13]. It should be noted that the MIXCRA-retrieved optical depths are converted to visible optical depths and, thus, are directly comparable with the HSRL-derived values.

### B. HSRL

The HSRL deployed during the M-PACE is an advanced automated lidar system that was designed for operation in the Arctic environment [14]. The HSRL transmits pulses of polarized light at 532 nm into the atmosphere at a repetition rate of 4 kHz using a “transceiver” design, where laser beam is expanded by the telescope that collects the backscattered signal. The HSRL records the backscatter from the atmosphere in two channels: one that records the entire Rayleigh–Mie return (the aerosol plus molecular, or combined, channel) and one that records this return with the central portion removed by an iodine absorption filter. The iodine filter essentially removes the backscatter associated with aerosol and cloud particles in the atmosphere, and hence, the measured return is purely a molecular backscattered signal. The change in the slope of the molecular signal relative to a clear sky atmosphere is due to the extinction by the aerosol or cloud particles [14], and thus, the HSRL provides a direct measurement of the cloud extinction profile. This profile is then integrated from cloud base to cloud top to provide the optical depth of the cloud. The accuracy of the extinction profile, particularly in the near range (lowest 1–2 km), is sensitive to the accuracy of the corrections that are used to account for the receiver/transmitter “overlap” and the afterpulsing characteristic of the detection electronics.

The key aspect to the HSRL is finely tuning the outgoing laser wavelength such that it transmits at exactly the same frequency that is absorbed by the iodine cell that is used to remove the particulate component in the molecular channel. This is accomplished via active seeding of the laser and using a servo loop that locks the laser wavelength to the iodine absorption line.

Since the HSRL transmits at 532 nm, which is near the maximum of the solar radiation at the Earth’s surface, etalon filters are used to only select the desired wavelength region of interest to send to the detectors. The use of these filters results in an excellent signal-to-noise ratio in the HSRL for 30-m 30-s resolution.

The HSRL is also polarization sensitive, and thus, it is able to provide profiles of linear depolarization ratio with altitude. These profiles are useful for determining cloud phase, as spherical particles, such as suspended cloud droplets, have low depolarization ratios (less than 5%), whereas nonspherical ice particles have significantly larger depolarization ratios [15].

### III. RESULTS

We desired to identify single-layer mixed-phase clouds from the M-PACE period to evaluate the MIXCRA-retrieved ice and liquid optical depths with the directly measured optical depths from the HSRL. For purposes of this discussion, a single-layer mixed-phase cloud is defined as in [3]: “a complete cloud system that contains both liquid and ice when viewed vertically, and it is not necessary for all volumes to be filled with both ice and liquid.” The depolarization ratio from the HSRL provides an indication of the dominant shape in the lidar volume (spherical liquid droplets or nonspherical ice particles), and thus, we assign each lidar volume as either ice or liquid. We focused on cloud systems where a single layer of predominantly supercooled liquid at the top was precipitating ice underneath. Thus, the integrated extinction from the surface to cloud base yielded the optical depth of the ice, whereas the integration of the extinction from the liquid cloud base, which is easily identified in the lidar backscatter and depolarization-ratio profiles, to cloud top provides the optical depth of the liquid. Sensitivity studies have demonstrated that the infrared retrievals are relatively insensitive to the vertical distribution of the ice and liquid in the cloud layer (i.e., ice over liquid, liquid over ice, or both ice and liquid in the same volume) as long as the cloud temperature profile is correct [7]; therefore, we feel that this validation in “simple” cases like the ones shown here will extend to more complex single-layer cloud scenes.

Unfortunately, the M-PACE period was warmer than usual, which is relative to climatology, and thus, many of the clouds over the NSA were too optically thick to be fully profiled by the lidar [5]. If the cloud is too optically thick, the outgoing laser energy is fully attenuated before reaching the top of the cloud (the lidar will be fully attenuated if the optical depth is more than three to four), and thus, the integral of the cloud extinction from the HSRL will underestimate the true optical depth. The maximum total optical depth that can be retrieved from MIXCRA in the configuration used here is approximately six [4], and thus, the data are selected only if the lidar is able

TABLE II  
TIME PERIODS FROM NOVEMBER 2004 INCLUDED IN THE ANALYSIS

Date	Time Range [UTC]	Avg. PWV [mm]
01	1800 – 2400	2.2
02	0600 – 0900	2.3
02	2000 – 2200	2.2
03	1600 – 2000	2.3
05	2100 – 2230	3.4
06	0900 – 1500	2.8
10	0130 – 0400	2.1
10	0630 – 0900	2.6
10	1330 – 1430	2.5

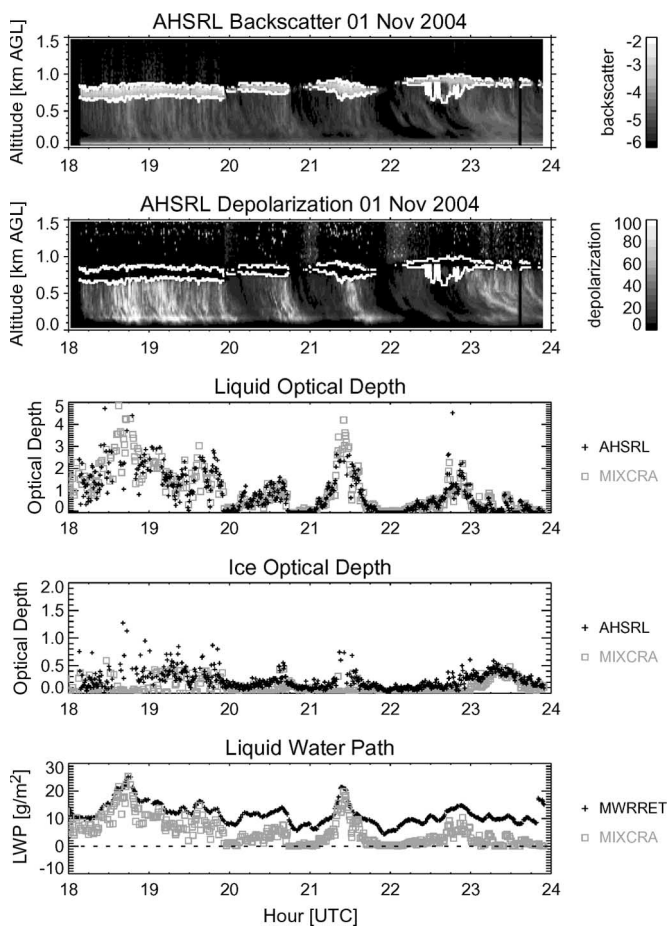


Fig. 1. Data from November 1, 2004, showing the time-height backscatter and depolarization cross sections from the HSRL, the optical depth of the liquid and ice components of the mixed-phase cloud derived from the HSRL and retrieved using MIXCRA, and the LWP retrieved using MIXCRA and MWRRET.

to fully profile the cloud. Several excellent cases were observed in early November 2004 before the HSRL was removed from the NSA site. Table II lists the dates and times of the cases analyzed here.

The results from November 1 and 2 are shown in Figs. 1 and 2, respectively; the backscatter from the combined channel and the depolarization ratio observed by the lidar, the time series of optical depth of the liquid and ice components derived from the lidar extinction and MIXCRA retrievals, and the liquid water path (LWP) retrieved by MIXCRA is compared with the advanced microwave radiometer retrieval (MWRRET) algorithm [13]. The base and the top of the liquid water layer are overplotted in the top two panels as white lines. There is an excellent qualitative agreement between the liquid and ice opti-

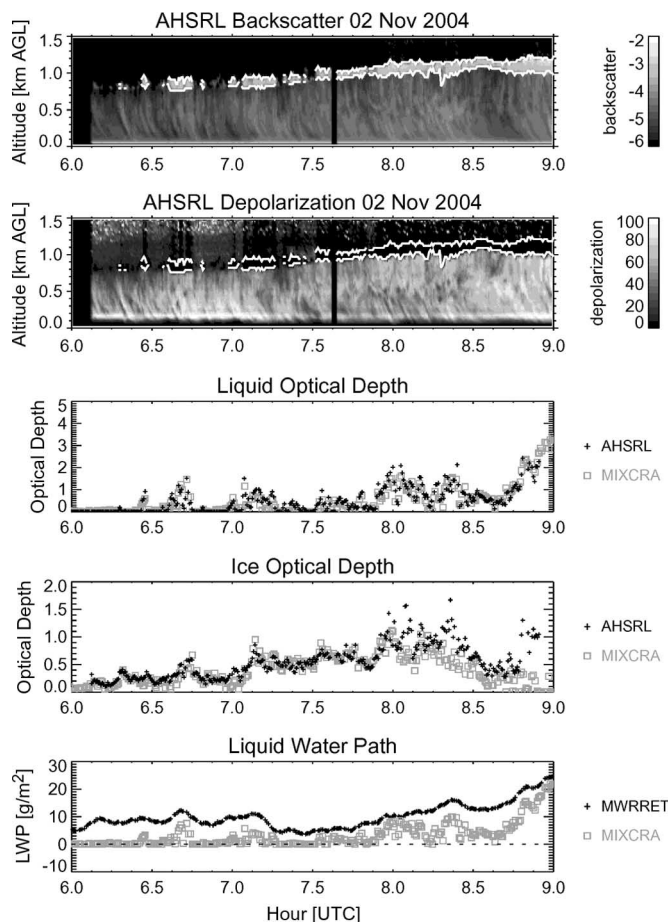


Fig. 2. Same as Fig. 1 for November 2, 2004.

cal depths derived from the lidar and retrieved by MIXCRA, as the MIXCRA results follow the change in the cloud properties as indicated by the lidar very well. The MIXCRA LWP is considerably more accurate than the MWRRET-retrieved value, as the MWRRET values show positive biases even during periods where no liquid water cloud was identified in the lidar data (such as between 6.0–6.25 UTC and 6.8–6.9 UTC on November 2).

A direct quantitative comparison of the MIXCRA-retrieved and HSRL-derived optical depths is challenging due to the differences in averaging interval (30 s for the lidar versus 12 s every 25 s for the AERI) and the differences in field of view (45  $\mu$ rad for the lidar versus 46 mrad for the AERI). We have interpolated the HSRL optical depth data to the AERI sample times, realizing that this approach will add some scatter to the comparison but should not affect the bias. The scatter plots of the ice and liquid optical depths for the periods in Table II are shown in Fig. 3, with bias and rms results provided in Table III. The scatter plot of ice optical depth data shows a fair correlation of  $r = 0.647$  between the two techniques. Furthermore, the relative sensitivity, as determined by the slope of the data on this log–log plot, shows a very similar sensitivity to ice between the two techniques with a slope of 1.055. Some of this variability is likely due to the assumption of a single ice particle habit (shape) in the MIXCRA retrieval as well as the differences in field of view and averaging period. The agreement in the liquid water optical depths between the two

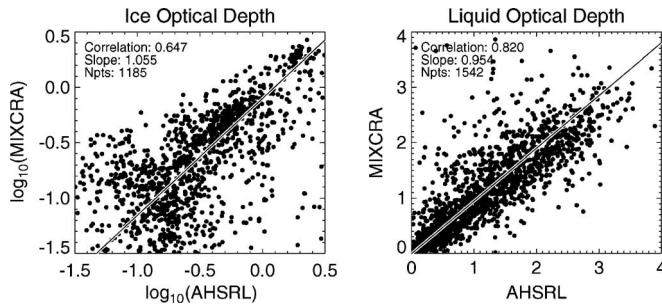


Fig. 3. Scatter plot of optical depth from the HSRL versus MIXCRA for (left) the ice and (right) liquid components of the mixed-phase clouds in Table II.

TABLE III  
OPTICAL-DEPTH COMPARISON STATISTICS BETWEEN THE  
HSRL AND THE MIXCRA RETRIEVALS

Range <sup>†</sup>	Water			Ice		
	Bias	RMS	N	Bias	RMS	N
0.00-0.10	-0.16	0.54 <sup>#</sup>	51	-0.08	0.13	155
0.10-0.25	-0.11	0.38	129	0.02	0.12	389
0.25-0.50	-0.04	0.39	189	0.06	0.19	289
0.5-1.0	-0.04	0.46	331	0.15	0.33	208
1.0-2.0	0.05	0.51	524	0.43	0.70	103
2.0-3.0	0.34	0.56	285	1.15	1.45	39
3.0-4.0	0.69	0.83	33	1.70	1.78	2

<sup>†</sup>HSRL data were used to select the points in each optical depth range bin

<sup>#</sup>The interquartile spread for this bin is 0.08; for all other water and ice optical depth bins the interquartile spread was within a factor of 2 relative to the RMS.

methods is better than the ice, with a correlation coefficient of  $r = 0.820$  and a slope of 0.954. For cases where the optical depth was less than one, the bias in the MIXCRA optical depths was smaller than 0.16 relative to the HSRL. However, both the bias and the rms increased as the optical depth of the cloud (as determined by the lidar) increased above two; this is likely due to the difficulty in determining when the HSRL is fully attenuated in these optically thicker cases.

In this letter, we have made the assumption that there is only liquid or ice in each lidar volume in order to derive the optical depths of each component from the HSRL data. While this may be largely true in the precipitation region of the cloud from which the ice optical depth is derived, the liquid portion of the cloud almost certainly contains some ice particles, as these grow in the supercooled liquid water environment and then fall from the base of the cloud as ice precipitation. We are unable to determine directly from the HSRL data how much ice may be in the predominantly liquid cloud. However, the inclusion of the ice optical depth in the lidar estimation of the liquid optical depth would result in a slight overestimation of the true liquid water optical depth, and the sensitivity to liquid water optical depth of the MIXCRA algorithm to the true liquid water optical depth may be even better.

#### IV. CONCLUSION

This letter represents the first direct evaluation of the accuracy of the MIXCRA-retrieved optical depths in mixed-phase clouds. Over 1000 cases of mixed-phase clouds observed during the M-PACE demonstrate that the MIXCRA-retrieved liquid optical depths are in good agreement with the HSRL-derived values (slope of 0.954) and that the ice optical depths

between the two approaches are also in good agreement (slope of 1.055). These results, together with the previous evaluation of MIXCRA in liquid-only clouds [12], indicate that the MIXCRA-retrieved results are accurate and provide justification for an analysis of the long time series of cloud properties derived from this algorithm at the NSA site.

#### ACKNOWLEDGMENT

The authors would like to thank the Atmospheric Radiation Measurement (ARM) Program for collecting the data analyzed in this letter and Dr. J. Verlinde and his NSA site scientist team for the organization and successful conduction of M-PACE. The authors would also like to thank J. Voyles and the ARM Program management for including the HSRL in M-PACE and the members of the University of Wisconsin Lidar Group, namely, Dr. I. Razenkov, J. Garcia, and J. Hendrick, for their work in installing and operating the HSRL at the NSA site.

#### REFERENCES

- [1] J. M. Comstock *et al.*, "An intercomparison of microphysical retrieval algorithms for upper tropospheric ice clouds," *Bull. Amer. Meteorol. Soc.*, vol. 88, no. 2, pp. 191–204, Feb. 2007.
- [2] D. D. Turner *et al.*, "Thin liquid water clouds: Their importance and our challenge," *Bull. Amer. Meteorol. Soc.*, vol. 88, no. 2, pp. 177–190, Feb. 2007.
- [3] M. D. Shupe, J. S. Daniel, G. de Boer, E. W. Eloranta, P. Kollias, C. N. Long, E. Luke, D. D. Turner, and J. Verlinde, "A focus on mixed-phase clouds: The status of ground-based observational methods," *Bull. Amer. Meteorol. Soc.*, 2007, to be published.
- [4] D. D. Turner, "Arctic mixed-phase cloud properties from AERI lidar observations: Algorithm and results from SHEBA," *J. Appl. Meteorol.*, vol. 44, no. 4, pp. 427–444, Apr. 2005.
- [5] J. Verlinde *et al.*, "The mixed-phase arctic cloud experiment (M-PACE)," *Bull. Amer. Meteorol. Soc.*, vol. 88, no. 2, pp. 205–221, Feb. 2007.
- [6] K. Stammes, R. G. Ellingson, J. A. Curry, J. E. Walsh, and B. D. Zak, "Review of science issues, deployment strategy, and status for the ARM north slope of Alaska—Adjacent arctic ocean climate research site," *J. Clim.*, vol. 12, no. 1, pp. 46–63, Jan. 1999.
- [7] D. D. Turner, S. A. Ackerman, B. A. Baum, H. E. Revercomb, and P. Yang, "Cloud phase determination using ground-based AERI observations at SHEBA," *J. Appl. Meteorol.*, vol. 42, no. 6, pp. 701–715, Jun. 2003.
- [8] R. O. Knuteson *et al.*, "Atmospheric emitted radiance interferometer. Part I: Instrument design," *J. Atmos. Ocean. Technol.*, vol. 21, no. 12, pp. 1763–1776, Dec. 2004.
- [9] R. O. Knuteson, "Atmospheric emitted radiance interferometer. Part II: Instrument performance," *J. Atmos. Ocean. Technol.*, vol. 21, no. 12, pp. 1777–1789, Dec. 2004.
- [10] D. D. Turner, R. O. Knuteson, H. E. Revercomb, C. Lo, and R. G. Dedecker, "Noise reduction of atmospheric emitted radiance interferometer (AERI) observations using principal component analysis," *J. Atmos. Ocean. Technol.*, vol. 23, no. 9, pp. 1223–1238, Sep. 2006.
- [11] D. D. Turner and R. E. Holz, "Retrieving cloud fraction in the field-of-view of a high-spectral-resolution infrared radiometer," *IEEE Geosci. Remote Sens. Lett.*, vol. 2, no. 3, pp. 287–291, Jul. 2005.
- [12] D. D. Turner, "Improved ground-based liquid water path retrievals using a combined infrared and microwave approach," *J. Geophys. Res.*, vol. 112, no. D15, D15 204, 2007. DOI:10.1029/2007JD008530.
- [13] D. D. Turner, S. A. Clough, J. C. Liljegren, E. E. Clothiaux, K. Cady-Pereira, and K. L. Gaustad, "Retrieving liquid water path and precipitable water vapor from the atmospheric radiation measurement (ARM) microwave radiometers," *IEEE Trans. Geosci. Remote Sens.*, vol. 45, no. 11, pp. 3680–3690, Nov. 2007.
- [14] E. W. Eloranta, "High spectral resolution lidar," in *Lidar: Range-Resolved Optical Remote Sensing of the Atmosphere*, K. Weitkamp, Ed. New York: Springer-Verlag, pp. 143–163.
- [15] K. Sassen, "The polarization lidar technique for cloud research: A review and current assessment," *Bull. Amer. Meteorol. Soc.*, vol. 72, no. 12, pp. 1848–1866, Dec. 1991.